Charge-injection instability in perfect insulators

Thomas Christen
ABB Corporate Research Ltd., CH-5405, Baden-Dättwil, Switzerland
(Received 10 March 1997)

We show that in a macroscopic perfect insulator, charge injection at a field-enhancing defect is associated with an instability of the insulating state or with bistability of the insulating and the charged state. The effect of a nonlinear carrier mobility is emphasized. The formation of the charged state is governed by two different processes with clearly separated time scales. First, due to a fast growth of a charge-injection mode, a localized charge cloud forms near the injecting defect (or contact). Charge injection stops when the field enhancement is screened below criticality. Secondly, the charge slowly redistributes in the bulk. The linear instability mechanism and the final charged steady state are discussed for a simple model and for cylindrical and spherical geometries. The theory explains an experimentally observed increase of the critical electric field with decreasing size of the injecting contact. Numerical results are presented for dc and ac biased insulators. [S0163-1829(97)01231-9]

I. INTRODUCTION

Insulation of dielectrics is limited due to dielectric breakdown.[1–3] There exist several different physical mechanisms that lead to instabilities associated with dielectric breakdown at high electric fields, e.g., thermal runaway and impact ionization avalanches. At breakdown, a change from an insulating to a conducting state occurs, at least in a certain spatial region and for a certain time. A release of charge carriers is possible from two different sources. First, carriers can be generated intrinsically via a bulk instability, e.g., by ionization of impurities. Secondly, carriers can enter due to injection at the electrodes. In this paper, we show that charge injection is associated with an instability too. In contrast to bulk instabilities, however, charge injection is a boundary instability where the unstable mode (charge injection mode) is localized at the injecting contact.

In practice, charge injection in macroscopic insulating bodies occurs at geometrical defects of the electrodes where the electric field can be strongly enhanced. Below we will consider concentric cylindrical and spherical contact geometries. A small inner electrode has a large electric field and can serve as a model for a field enhancing defect. The cylindrical system describes also a coaxial cable filled with a dielectric medium, which is of obvious technical interest.

Charge injection in dielectrics has been investigated experimentally for a tip-plate geometry by Hibma and Zeller,[4] and has been modeled by Zeller and Schneider[5] in the limit of an infinitely sharp mobility edge and by neglecting diffusion. They describe the mobility edge with a mobility $\mu(E)$, which vanishes for $E<E_c$ but which is very large for $E>E_c$, where E_c is a critical value of the electric field ($\approx 10^7$ V/cm). In this model a space charge forms near the tip when the local field reaches the mobility edge. The space charge, in turn, screens the electric field enhancement at the tip and pins it to the mobility edge (field limiting space charge). Zeller and collaborators assume a bulk instability at E_c associated with an S-shaped negative differential conductivity, which forms the basis of their theory.[5,6] Below we show, however, that there is no need for such an underlying bulk instability. Charge injection turns out to be an instability by itself.

Boggs[7,8] pointed out the usefulness of the screening by the injected space charge in ac driven field-grading materials. His model, however, is based on the concept of conductivity, which cannot lead to a consistent physical description of charge injection. The theory assumes a conductivity that is only a function of the field and that does not distinguish between intrinsic and injected charge carriers. Note that charge injection is a boundary effect, while conductivity is a bulk quantity associated with intrinsic rather than with injected carriers. Boggs' approach leads, nonetheless, to qualitatively correct ac results in the limit of an infinitely sharp mobility edge and in a certain frequency regime.

For the sake of clearness, we consider a perfect insulator, which is defined here as a dielectric without intrinsic carriers and with a constant permittivity $\epsilon\ (=\epsilon_r,\epsilon_0)$. Electrons or holes can be present only due to injection at the electrodes. Without charge injection, a voltage difference at the contacts induces a charge that is located outside the dielectric in a thin surface layer (with a thickness of the very short Debye length) of the metal contacts. We call this locally neutral state of the insulator the *ideal insulating state*. The electric field in the insulator is then uniquely determined by the Laplace equation. The electric field at the contacts is fully determined by the potential differences of the contacts. Clearly, this situation corresponds to a purely capacitive arrangement of the contacts in a dielectric medium.

A prescription of arbitrary boundary conditions to the electric field at the contacts (e.g., $E=0$) is more restrictive and in general implies the presence of a space charge in the dielectric medium. The field is then determined by the Poisson equation. Important work on charge injection[1,9–12] treats the formation of a space charge in this way as a direct consequence of boundary conditions. These theories treat the charged state, but they do not consider the stability of the locally neutral state.

A different approach, which is appropriate for metal-semiconductor contacts, is to prescribe a Richardson-Schottky[13,14] or a Fowler-Nordheim[15,16] current-

field characteristic in order to model thermionic (field) emission or a tunneling current through the contact barrier, respectively. In contrast to the well-defined metal-semiconductor microcontacts manufactured by a highly developed semiconductor technology, macroscopic metal-insulator contacts used in high-voltage devices are not well defined. A description on a hydrodynamic level is thus more appropriate than a treatment on a microscopic level. Therefore, we will prescribe below boundary conditions to the charge density ρ. For homogeneous boundary conditions, it turns out that the locally neutral state ($\rho \equiv 0$) is always a stationary solution of the problem. However, we will show that this ideal insulating state can become unstable against a charge injecting mode or that bistability of neutral and charged state can occur.

This paper is organized as follows. In the next section, we introduce a model for the perfect insulator with phenomenological boundary conditions. In Sec. III, we investigate the charge injection instability of the ideal insulating state. The steady state that eventually develops is discussed in Sec. IV. Finally, in Sec. V, we present numerical results for an ac biased perfect insulator.

II. THE MODEL

We consider a material with electron-hole symmetry and with an immediate recombination of electrons (n) and holes (p) by annihilation. This means that the mobilities and the diffusion constants of electrons and holes have equal absolute values, $\mu \equiv -\mu_n \equiv \mu_p$, and $D \equiv D_n \equiv D_p$, respectively. The Einstein relation is not considered for the present nonequilibrium system, and we assume that D is a field-independent constant. Due to the fast electron-hole recombination, the carrier density is equal to the absolute value of the charge density. The drift current is then simply given by $\mu(E)|\rho|E$. Dynamic equations for electrons and holes describing generation-recombination processes do not appear. We emphasize that, except for the ac results, all results below are valid also for unipolar conduction and are not consequences of the electron-hole symmetry and of the fast recombination. In particular, the injection instability discussed below occurs for unipolar conduction. In this case, e.g., $\rho \geqslant 0$ and the drift current reads $\mu(E)\rho E$.

Consider now a perfect insulator in a capacitor of cylindrical or of spherical symmetry. Metal contacts are attached at the inner and the outer radius, r_1 and $r_2 (\gg r_1)$, respectively. In the following, the cylindrical capacitor of length L_z and the spherical capacitor are labeled with $d=1$ and $d=2$, respectively. All quantities depend only on the radial coordinate, r. The (radial) current density can be expressed in terms of the charge density ρ and the (radial) electric field E:

$$j = \mu(E)|\rho|E - D\partial_r \rho. \tag{1}$$

We assume a mobility $\mu(E)$ that depends on the field in the form $\mu(E)E \equiv v|E/E_0|^{\alpha}\mathrm{sgn}(E)$, where $\alpha \geqslant 1$ is a measure of nonlinearity and where v is a positive velocity. A power-law current-field relation usually describes very well the behavior near insulator-conductor transitions at high fields. It is a difficult problem to relate the phenomenological parameters α and v to microscopic quantities in typical insulating materials used in high-voltage devices (e.g., ceramics, polymers). There are, however, special cases, where exponents characterizing the nonlinearity of the current response have been determined from microscopic models.[17]

The limit $\alpha \to \infty$ corresponds to the infinitely sharp mobility edge at $E = E_0$ discussed in Ref. 5. Note that already the case of a constant mobility ($\alpha = 1$) corresponds to a nonlinear current-field relation since ρ is related to the electric field via the Poisson equation

$$\epsilon \nabla E = \rho. \tag{2}$$

Consequently, a linear dielectric relaxation mode does not exist in the perfect insulator.

There are two equivalent formulations of the dynamics, namely, in terms of the Maxwell equation

$$\epsilon \partial_t E = \nabla \times H - j, \tag{3}$$

which is a dynamic equation for the electric field, or in terms of the continuity equation,

$$\partial_t \rho = -\nabla j, \tag{4}$$

which is a dynamic equation for the charge density. For convenience, below we use Eq. (3) for the numerical simulations and Eq. (4) for the analytical discussion.

The system is driven electrically via a coupling to an external electric circuit, which consists here of a voltage bias $V(t)$ and an Ohmic resistor R_{ext} in series. The total (radial) current density $(\nabla \times H)_r = J/r^d$ is determined by

$$J = a_d \left(V(t) - \int_{r_1}^{r_2} E dr \right), \tag{5}$$

where $a_1 = (2\pi L_z R_{\mathrm{ext}})^{-1}$ and $a_2 = (4\pi R_{\mathrm{ext}})^{-1}$ for the cylindrical and the spherical case, respectively. We mention that Eq. (5) gives rise to a strong nonlocality, which can influence qualitatively the spatiotemporal dynamics of the system.[18] Below, we restrict ourselves to the limit case of voltage control, i.e., $R_{\mathrm{ext}} \to 0$ and to low frequencies such that inductive effects can be neglected. An increase of R_{ext} corresponds to forcing a current, which requires the presence of charge and is thus expected to lower the stability of the ideal insulating state. Voltage control can equivalently be expressed in the form $V(t) = \int_{r_1}^{r_2} E dr$.

In order to have a well-defined problem we specify mixed homogeneous boundary conditions to the charge density

$$\partial_r \rho|_{r_{1,2}} \pm \kappa \rho|_{r_{1,2}} = 0, \tag{6}$$

where κ is a phenomenological parameter, and where $+$ and $-$ refer to r_1 and r_2, respectively. Some remarks concerning this boundary condition are in order. First, a restriction to homogeneous boundary conditions is not necessary. An additional inhomogeneity in Eq. (6) leads to a finite boundary charge. In this paper, however, we want to show that charge injection occurs even for homogeneous boundary conditions where a locally neutral state exists. Secondly, κ can depend on the local electric field. Such nonlinear boundary conditions can lead to instabilities. Below we show that even for the linear case an instability occurs, and we discuss the behavior of the perfect insulator as a function of κ. We men-

tion that phenomenological parameters introduced in (inhomogeneous and nonlinear) boundary conditions are, in principle, related to microscopic quantities. This is analogous to the formulation of hydrodynamic boundary conditions starting from, e.g., the Boltzmann transport equation. However, this problem goes beyond the subject of this work.

Thirdly, we assume that the charge does not ''wet'' the contacts, i.e., $\kappa \leqslant 0$. This is reasonable if the microscopic contact potential has the shape of a barrier. In a purely diffusive system, a ''wetting'' density leads to an instability of the uniform state. For homogeneous Neumann boundary conditions ($\kappa = 0$) that describe contacts with vanishing diffusion current, the ideal insulating state in the diffusive regime is marginally stable (gapless stability spectrum). Indeed, an arbitrary spatially uniform ρ is a solution in the linear diffusive regime, which implies the existence of a zero mode. For finite negative κ, the $\rho \equiv 0$ state is stable in this regime. In the following section we show that, on the other hand, an instability of the ideal insulating state occurs in the drift dominated regime.

III. INSTABILITY OF THE IDEAL INSULATING STATE

In this and the following section, we consider a stationary and positive bias voltage applied to the contacts, $V(t) \equiv V > 0$. Obviously, a steady state of the system is given by $\rho \equiv 0$ and $E = C_d / r^d$ with $V/C_1 = \ln(r_2/r_1)$ and $V/C_2 = r_1^{-1} - r_2^{-1}$. This ideal insulating state corresponds to a purely capacitive system. To test the linear stability of this state, we seek for the dynamics of a weak perturbation $(\delta E, \delta\rho) \propto \exp(\lambda t)$, which satisfies the boundary conditions (6). From the continuity equation (4), one finds an eigenvalue equation for the growth rate λ:

$$\lambda\,\delta\rho + \frac{1}{r^d}\partial_r\left(\frac{(C_d/E_0)^\alpha}{r^{d(\alpha-1)}} v\,|\delta\rho| - D r^d \partial_r \delta\rho\right) = 0. \qquad (7)$$

An instability of the ideal insulating state occurs if there exists an eigenvalue λ with a positive real part, since the mode $\delta\rho$ associated with such a λ grows exponentially in time. A dimensional analysis of Eq. (7) leads to a ''scaling relation'' for the growth rate,

$$\lambda = \frac{D}{r_1^2} f(\Lambda), \qquad (8)$$

where $\Lambda = (r_1 v/D)(E_1/E_0)^\alpha$ has the meaning of a dimensionless control parameter. Here, $E_1 = C_d/r_1^d$ is the electric field at the inner contact. Note that the function f depends still on d, α, κr_1. The dependence on κr_2 is weak for $r_1 \ll r_2$ and will be suppressed whenever possible. The critical field at instability depends on the various parameters in the form

$$E_c = E_0 \sqrt[\alpha]{\frac{D}{r_1 v}\Lambda_c(\alpha, d, \kappa r_1)}, \qquad (9)$$

where the function Λ_c has to be determined from $f = 0$. The eigenvalue λ with the largest real part turns out to be purely real and can be estimated if either the diffusion current or the drift current dominates. First, if the drift term can be neglected, Eq. (7) reduces to a linear diffusion equation. Consequently, the eigenfunctions of the stability problem are of diffusion type and are damped or marginally stable, provided $\kappa \leqslant 0$. On the other hand, if the diffusion term can be neglected, the stability problem reduces to a first order differential equation. Solving Eq. (7) at $D = 0$ leads to a growth rate

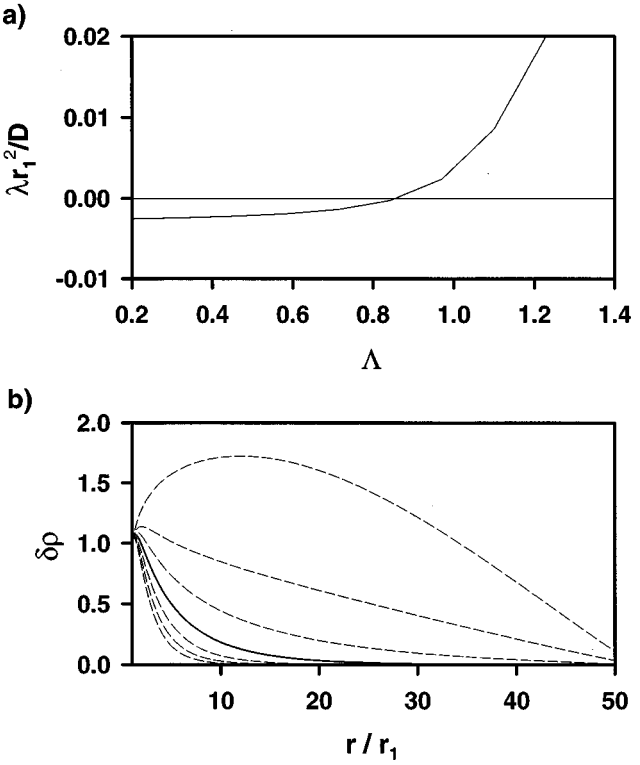

FIG. 1. (a) Largest eigenvalue λ of the stability problem as a function of the control parameter Λ ($\kappa r_1 = -0.5$ $d = 1$, $\alpha = 3$). (b) Eigenfunctions of the stability problem. The solid curve represents the marginal charge-injection mode ($\lambda = 0$) at $\Lambda = \Lambda_c$. Modes are more localized at the inner contact as Λ increases.

$$\lambda = \frac{v}{r_1}\left(\frac{E_1}{E_0}\right)^\alpha [d(\alpha-1) + r_1\kappa], \qquad (10)$$

which indicates an instability associated with a perturbation

$$\delta\rho(r) \propto r^{d(\alpha-1)} \exp\left[-\left(\frac{r}{r_1}\right)^{d\alpha+1} \frac{d(\alpha-1)+r_1\kappa}{d\alpha+1}\right]. \qquad (11)$$

Equation (11) describes the injection mode, which is localized at the inner contact. Obviously, a negative κ acts to slow down the growth of the unstable mode. In Fig. 1, numerical solutions of the stability problem of the cylindrical case ($d = 1$) are shown as a function of Λ with $\kappa r_1 = -0.5$. For $D/(v r_1) \to 0$ and $\lambda \geqslant 0$, the numerical results are in good accordance with the approximate analytical results (10) and (11).

The physical mechanism for the instability can be understood as a positive feedback process. Consider a large electric field at $r = r_1$, and assume a negative field fluctuation, $\delta E < 0$ with $\partial_r \delta E > -\delta E/r_1$, localized at r_1. The Poisson equation implies then a positive charge fluctuation $\delta\rho$ at this contact. Using the linearized Maxwell equation,

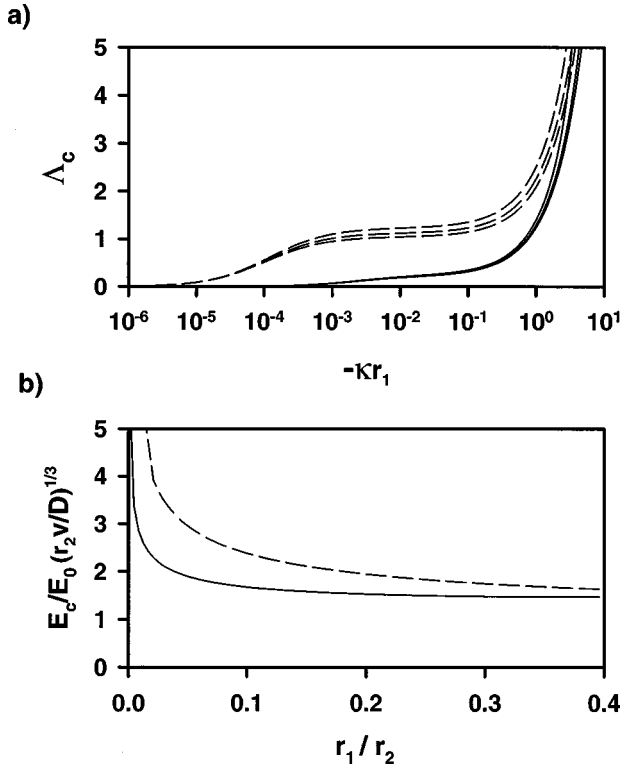

FIG. 2. (a) Critical values Λ_c as functions of $-\kappa r_1$, for cylindrical (solid) and spherical (dashed) geometries ($r_1/r_2=0.01$). Different curves with decreasing stability threshold belong to $\alpha=3$, 5, and 15. (b) Critical value of the electric field at the inner electrode as a function of the size of the injecting electrode ($\alpha=3$; solid: $d=1$, dashed: $d=2$).

$\epsilon\partial_t \delta E \approx -\delta j<0$, one concludes that the negative field fluctuation grows in amplitude, if drift dominates diffusion. The initial perturbation is thus amplified, which characterizes an instability. We mention that for $\alpha=1$, the charge injection mode (11) has no physical meaning. In this case, the ideal insulating state is linearly stable, although it is not necessarily globally stable.

For finite D, a competition between the stabilizing diffusion term and the destabilizing drift term leads to a finite critical value of the control parameter Λ_c or, equivalently, to a finite critical field E_c. In order to discuss the dependence of Λ_c in Eq. (9) on κr_1, we solve Eq. (7) at $\lambda=0$. A solvability condition leads then to an expression for κr_1 as a function of Λ_c (Appendix). The result is plotted in Fig. 2(a) for various values of the nonlinearity parameter α, for $d=1,2$, and for constant radii. Clearly, Λ_c vanishes for $\kappa\to 0$. On the other hand, the locally neutral state becomes more stable as $-\kappa$ increases which is due to a decrease of the charge density of a density fluctuation at the injecting contact.

In a similar way, stability analysis yields the critical field E_c as a function of r_1. We find that the critical field is almost independent of r_1 except for small r_1, where E_c becomes large. This behavior is more pronounced as α increases. For $\alpha=3$ and $d=1,2$, the results are shown in Fig. 2(b). For a tip-plate geometry, Hibma and Zeller[4] found experimentally that the critical field is almost independent of the tip size in a large range but increases considerably for very small tip radii. Our theory clearly reproduces this behavior.

IV. THE CHARGED STEADY STATE

The injection of the charge acts to decrease the field enhancement. Consequently, the growth of the injection mode saturates at a field below the critical value E_c. Zeller and Schneider[5] observed that in the infinitely sharp mobility-edge limit, $\alpha\to\infty$, the final state consists of a charged region with $\rho\propto 1/r$ and $E(r)\approx E_c$ for $r_1<r<\overline{r}$, and a locally neutral region, $\rho\equiv 0$ and $E\propto 1/r^d$, for $\overline{r}<r<r_2$. The outer radius $\overline{r}$ of the field limiting space charge is determined by the continuity of $E(r)$ at $\overline{r}$ and by the prescribed voltage drop, $V=\int E dr$. One expects for finite α (Ref. 5) and in the presence of diffusion that this state decays on a long time scale and is in fact part of a transient behavior. More concretely, the final charged steady state forms on two clearly separated time scales. On a short time scale determined by Eq. (8), charge is injected such that the electric field drops locally below the critical field. In a second step, the charge distributes slowly towards the new stable steady state. The associated time scale is approximately given by the transit time $\tau_{\rm tr}$ of the domain wall, which connects the charged and the neutral regions. A general discussion of front propagation into unstable states[19] goes beyond the purpose of this paper. Here, we give only a rough estimate for the transit time in the case of a thin domain wall

$$\tau_{\rm tr}\approx\frac{r_2}{v}\left(\frac{r_2 E_0}{V}\right)^{\alpha}. \tag{12}$$

In particular, we neglected diffusion, which acts to slow down the domain wall velocity and to smear out the domain wall. Equation (12) can be obtained by a projection onto the translation mode of the domain wall and has the simple interpretation that the front travels with the drift velocity of the carriers.

It should be noted that the slowness of the charge redistribution indicates a strong dependence on weak perturbations of the homogeneous insulator bulk. While weak forces are not expected to hinder the growth of the fast unstable injection mode, the charge redistribution can be considerably influenced by traps, grain boundaries, etc. Therefore an experimental observation of the slow dynamics and the final state discussed below requires a sufficiently clean material. Macroscopic insulating bodies used in high-voltage devices where the injection instability is expected to be most important are usually not very clean. Future models of the dynamics of the field limiting space charge should thus include bulk inhomogeneities.

In Fig. 3, we show a numerical simulation of charge injection in the perfect insulator for $d=1$ and $\alpha=3$. After an increase of the voltage beyond instability threshold, a charge domain forms. On a long time scale the charge cloud smears out and relaxes finally towards a $(1/r)$-like distribution, whereas the electric field becomes spatially uniform. In order to discuss this final steady state in the framework of our model, we first consider the case $D=0$. From $\nabla j=0$ one finds a bulk solution

$$E(r)=A_d r^{(1-d)/(1+\alpha)}, \tag{13}$$

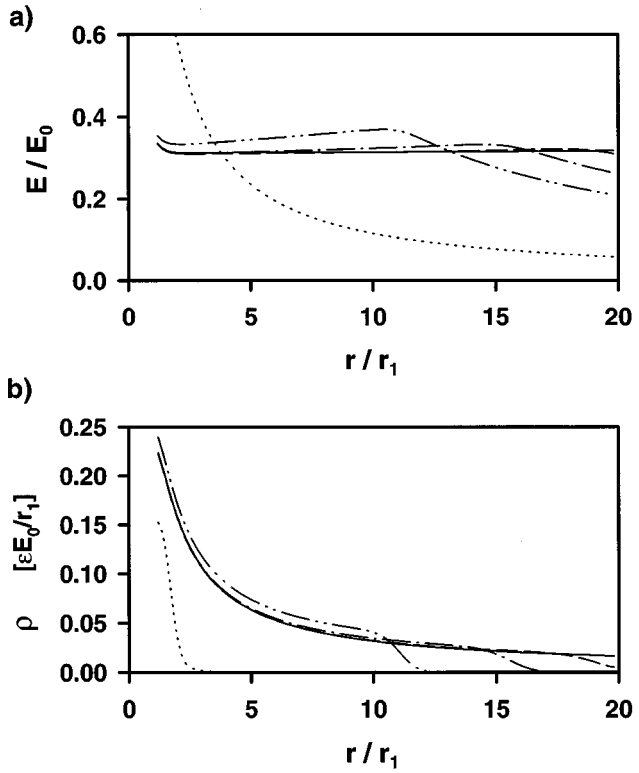

FIG. 3. Evolution of (a) the electric field distribution and (b) the charge density distribution beyond stability threshold. The localized injection mode (dotted curve) grows up to a certain amplitude. The domain wall moves into the bulk (dashed-dotted curves) until the final steady state with a uniform field (solid curve) is reached ($d=1$, $\alpha=3$).

$$\rho(r)=\epsilon A_d \frac{1+d\alpha}{1+\alpha} r^{-(\alpha+d)/(1+\alpha)}, \tag{14}$$

with $A_1=V/(r_2-r_1)$ and $A_2=V/(r_2^{\alpha/(1+\alpha)}-r_1^{\alpha/(1+\alpha)})/(1+\alpha^{-1})$ for the cylindrical and the spherical case, respectively. Note the similarity of the electric field distributions for $d=1$, α arbitrary, and for $\alpha\to\infty$, d arbitrary. In these cases, $E(r)$ relaxes eventually to a constant value [see also Fig. 3(a)].

Clearly, the bulk solution (14) does not satisfy the boundary conditions. For a small diffusion constant, the solution is expected to be changed considerably only in a boundary layer near the contacts. We find that the solution deep in the bulk far away from the contacts is only weakly disturbed by a small diffusion constant. For, e.g., the cylindrical geometry ($d=1$) and for $V<r_2E_0$, the bulk solution reads in leading order of D

$$E(r)=\frac{\tilde{V}}{r_2}\left[1-\frac{D}{\alpha v r}\left(\frac{r_2E_0}{\tilde{V}}\right)^{\alpha}\right], \tag{15}$$

where $\tilde{V}$ is determined by the prescribed voltage drop. For $d=\alpha=1$, Eq. (15) is the exact bulk solution. We recall that for $\alpha=1$ we do not find a linear instability of the ideal insulating state either numerically or with the analytical approximation (10). However, we conjecture bistability of neutral and charged state for $V>(D/\mu)\ln(r_2/r_1)$ and a loss of global stability at a certain field. Below, this conjecture will be confirmed with the help of a numerical simulation. A detailed investigation of this case, however, will be published elsewhere.

Assuming $r_2\gg r_1$, Eqs. (13) and (14) yield a current

$$I_d=b_d\epsilon v E_0\left(\frac{V}{r_2E_0}\right)^{\alpha+1}, \tag{16}$$

where $b_1=2\pi L_z$ and $b_2=4\pi r_2\alpha^{1+\alpha}(1+2\alpha)/(1+\alpha)^{2+\alpha}$ for the cylindrical and the spherical case, respectively. Slightly beyond instability threshold the current is finite, though it is small [of $O((r_1/r_2)^{\alpha+1})$]. We mention that for $d=2$, $\alpha=1$ and without diffusion, the $1/\sqrt{r}$ behavior of the electric field (13) has been discussed, e.g., by Lampert and collaborators.[9,10] Neglecting diffusion, they obtain a boundary layer due to an $E=0$ boundary condition at the contact. One recovers from Eq. (16) in this case the current-voltage characteristic of the perfect insulator in a spherical conductor, $I=(3/2)\pi\epsilon\mu V^2/r_2$. A detailed discussion of the steady state, e.g., in the presence of intrinsic carriers, can be found also in Refs. 9 and 10.

V. THE AC-DRIVEN INSULATOR

The localized field limiting space charge that forms at instability can be observed in ac experiments.[3,4] Since at instability λ depends exponentially on α, the injection mode grows very fast for large α. Consequently, in the limit of an infinitely sharp mobility edge ($\alpha\to\infty$) the electric field saturates immediately at $E\equiv E_c$ due to sceening. On the other hand, the characteristic time of the charge redistribution, Eq. (12), diverges, provided $E_cr_2>V$. For $E_cr_2<V$ the whole bulk is immediately charged up.

In the following, we consider a periodic voltage that vanishes for $t<0$ and that, for positive t, is given by $V(t)=\hat{V}\sin(\omega t)$. The frequency $\omega=2\pi/T$ obeys $\omega\tau_{\rm tr}\gg 1\gg\omega/\lambda$, where λ is the steady-state stability eigenvalue for an electric field E_1 equal to the amplitude of the electric field oscillation. Since $\lambda^{-1}\ll 1$ ms and the transit time $\tau_{\rm tr}$ is of the order of hours,[4] reasonable frequencies are in the range of $10^{-1}-10^3$ Hz.

Typical solutions are shown in Fig. 4 for the cylindrical geometry and for various values of α. The thin solid line represents the reference electric field E_1/E_0 at r_1 of the ideal insulating state with a purely capacitive response. The other curves represent numerical simulations of the ac response in the presence of injection. For fields below instability threshold, $E_1<E_c$, the sample remains locally neutral. An increase of the field beyond threshold leads to the injection of charge in such a way that the local electric field at the inner contact is saturated slightly below the critical field. Negative and positive charge is periodically injected for $\alpha=3$ (dotted curve). Clearly, due to the electron-hole symmetry the solutions are symmetric with respect to inversion of the sign of the amplitude. The critical field is about $2E_0$, where the field drops fast and saturates below E_0. This discontinuous transition from the neutral state to the charged state indicates

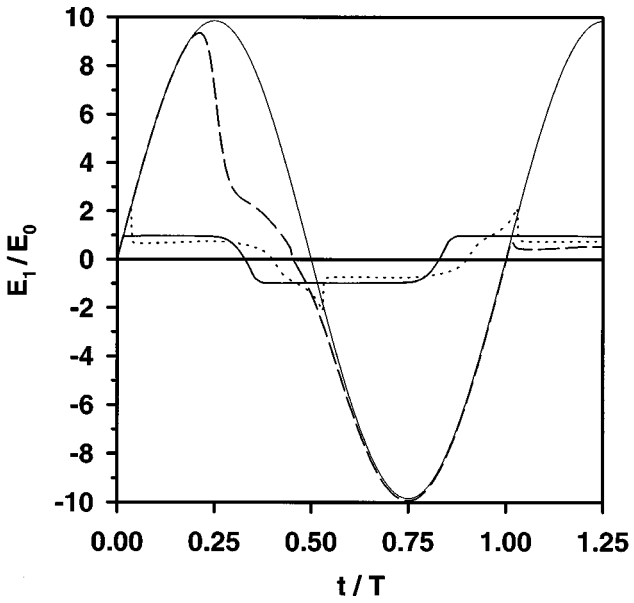

FIG. 4. Time dependence of the field at the inner electrode for $\alpha=1$ (dashed), $\alpha=3$ (dotted), and $\alpha=51$ (solid); $vr_1/D=0.1$. Solid thin curve: ac field without injection.

also bistability. In the limit of a sharp mobility edge (solid curve; $\alpha=51$), the neutral state decays immediately at $E_1=E_0$ and the electric field oscillates between $\pm E_0$, as expected.

On the other hand, for $\alpha=1$ the insulating state $\rho\equiv 0$ is linearly stable even for large amplitudes $\hat{V}$. For certain initial conditions or in the presence of additional current noise, however, we find also periodic solutions where only positive or only negative charge is injected. An example for positive charge injection is given by the dashed curve. Charge injection occurs at a large field amplitude $E_1\approx 9E_0$. Once charge has been injected, a part of it remains in the sample and decreases the value of the electric field (dashed curve) compared to the chargeless case (thin solid curve). During the negative half-cycle, the electric stress is thus enhanced. Due to the presence of this charge, a further injection occurs at a much lower field in the second cycle of the oscillation.

For initial conditions with reversed sign and $\hat{V}\rightarrow -\hat{V}$ we find injection of charge with different sign. We conclude that there are (at least) three different attractors, which indicates bistability in the stationary case. Consequently, even in a system with electron-hole symmetry, rectification is possible due to dynamical symmetry breaking via charge injection.

VI. CONCLUSION

We have investigated charge injection in a macroscopic and perfect insulator and for cylindrical and spherical geometries of the electrodes. The injecting metal-insulator contacts are modeled on a hydrodynamic level with boundary conditions for the charge density. We showed that, depending on the nonlinearity of the mobility, the ideal insulating state, $\rho\equiv 0$, is unstable against a charge injection mode at a critical field E_c. Former theories on charge injection assume either an intrinsic instability[6] or force injection directly by boundary conditions incompatible with a charge neutral state.[9,10] These theories cannot predict a finite critical field for the charge injection instability which is clearly observed in experiments[4]. For a macroscopic metal-insulator contact that is usually not well defined, phenomenological boundary conditions to the charge density (which serves as an order-parameter field) are appropriate. Our theory predicts not only a critical injection field E_c, but reproduces also the experimentally observed increase of E_c with decreasing radius of the injecting contact.[4]

For a constant mobility ($\alpha=1$), the ideal insulating state is linearly stable. But numerical ac simulations show a decay of the neutral state to a charged state. From this we conclude bistability and a loss of global stability of the ideal insulating state.

For $\alpha>1$, the time evolution from the insulating to the charged state occurs on two clearly separated time scales. On a short time scale, the injection mode grows at the instability and screens the electric field enhancement. A localized charge cloud forms near the contact. On a long time scale this charge redistributes over the whole sample. The localized field limiting space charge can be investigated with the help of an ac bias, which oscillates with a characteristic time lying between the just mentioned time scales.

Furthermore, we discussed the charged steady state for small diffusion constants. The current-voltage characteristics of these solutions are determined by the bulk properties and are thus equivalent to earlier results by Lampert and co-workers[9,10] in the perfect insulator limit.

Future work should address the following problems. First, the transport model must be refined to include additional physical effects such as the influence of intrinsic carriers, boundary states, traps, and impurity-band conduction, surface potential decay, and (bi-)polarons. The effect of traps enters already by part via the diffusion constant. A small intrinsic carrier density is expected to increase the stability of the neutral state due to a finite dielectric relaxation mode. Furthermore, electron-hole symmetry is not very realistic and one expects rectification in ac experiments.[20]

Of interest is also the inclusion of heat transport and the influence of the temperature, and of mechanical stresses. Another important task is the determination of the parameters appearing in the mobility-field relation and in the boundary conditions for the charge density from microscopic models. This is reasonable, however, only for microscopically well-defined bulk materials and metal-insulator contacts, which is usually not the case in typical high-voltage devices.

The following interesting problem concerns the case of a constant mobility without linear instability. Injection should then be associated with a nucleation of the charged phase at the contact,[21] probably via a critical droplet with a shape similar to the injection mode (11). Such an injection mechanism is also possible for bistability at $\alpha>1$ in the region where the ideal insulating state is supersaturated.

Finally, in order to quantitatively compare theoretical results with applications and experimental results, one should investigate geometries different from cylindrical and spherical symmetry such as, e.g., a tip-plate arrangement.[5,22,23] In contrast to the simple finite difference methods used in the simulations of this work, finite element methods are more appropriate to simulate charge injection in two- or three-dimensional geometries with lower symmetry.

ACKNOWLEDGMENTS

I am grateful to J. Rhyner for many valuable discussions and for a careful reading of the manuscript. I thank F. Stucki for drawing my attention to the relevant literature.

APPENDIX

We calculate the relation between the critical value Λ_c and the boundary-condition parameter κ by solving Eq. (7) with the boundary condition (6) for $\delta\rho$ at $\lambda=0$. We can assume $\delta\rho>0$. Integration of Eq. (7) leads to

$$\frac{\Lambda_c}{r^{d\alpha}}\delta\rho-\partial_r\delta\rho=\frac{A_2}{r^d},$$

with a constant A_2. The general solution of this equation is

$$\delta\rho=\left(A_1-A_2\int^r\frac{d\tilde{r}}{\tilde{r}^d}\exp\left(\frac{\Lambda_c\tilde{r}^{1-\alpha d}}{\alpha d-1}\right)\right)\exp\left(\frac{\Lambda_c r^{1-\alpha d}}{1-\alpha d}\right).$$

Applying the boundary conditions (6) to this function yields two linear equations for the constants A_1 and A_2. The existence of a nontrivial solution requires the vanishing of the determinant associated with these equations. This condition can be written in the form $a\kappa^2+b\kappa+c=0$ with constants a,b,c depending on Λ. The solution for negative κ defines the stability boundary plotted in Fig. 2(a). In a similar way one calculates the dependence of E_c on r_1, which is shown in Fig. 2(b).

[1] J. J. O'Dwyer, *The Theory of Electrical Conduction and Breakdown in Solid Dielectrics* (Clarendon Press, Oxford, 1973).

[2] L. A. Dissado and J. C. Fothergill, *Electrical Degradation and Breakdown in Polymers* (Peter Peregrinus Ltd., London, 1992).

[3] H. R. Zeller *et al.*, in *Festkörperprobleme Vol. 27* (Vieweg, Braunschweig, 1987), p. 223.

[4] T. Hibma and H. R. Zeller, J. Appl. Phys. **59**, 1614 (1986).

[5] H. R. Zeller and W. R. Schneider, J. Appl. Phys. **56**, 455 (1984).

[6] H. R. Zeller, IEEE Trans. Electr. Insul. **22**, 115 (1987).

[7] S. A. Boggs, IEEE Trans. Electr. Insul. **28**, 365 (1993).

[8] S. A. Boggs, IEEE Trans. Dielectr. Electr. Insul. **2**, 97 (1995).

[9] M. A. Lampert and P. Mark, *Current Injection in Solids*, (Academic Press, New York, 1970).

[10] M. A. Lampert and R. B. Schilling, in *Semiconductors and Semimetals*, edited by R. K. Willardson and A. C. Beer, Vol. 6 (Academic Press, New York, London, 1970) p. 1.

[11] N. F. Mott and R. W. Gurney, *Electronic Processes in Ionic Crystals* (Clarendon Press, Oxford, 1940).

[12] R. W. Hare, R. M. Hill, and C. J. Budd, J. Phys. D **26**, 1084 (1993), and references cited therein.

[13] O. W. Richardson, *The Emission of Electricity from Hot Bodies* (Longmans Geen and Co., London, 1921).

[14] W. Schottky, Phys. Z. **15**, 872 (1914).

[15] R. H. Fowler and L. Nordheim, Proc. R. Soc. London, Ser. A **119**, 173 (1928).

[16] E. L. Murphy and R. H. Good, Phys. Rev. **102**, 1464 (1956).

[17] G. Blatter and F. Greuter, Phys. Rev. B **33**, 3952 (1986).

[18] F. J. Elmer, Phys. Rev. A **41**, 4174 (1990); T. Christen, Z. Naturforsch. Teil A **50a**, 1128 (1995).

[19] W. van Saarloos, Phys. Rev. A **37**, 211 (1988); **39**, 6367 (1989).

[20] While epoxy resin shows a symmetric response, polyethylene is rectifying; T. Baumann *et al.* (unpublished).

[21] T. Christen, Europhys. Lett. **31**, 181 (1995).

[22] W. R. Schneider (unpublished).

[23] R. W. Hare and R. M. Hill, J. Phys. D **24**, 398 (1991).